Atmos. Meas. Tech. Discuss., https://doi.org/10.5194/amt-2017-222
Manuscript under review for journal Atmos. Meas. Tech.
Discussion started: 9 August 2017

Atmospheric Measurement Techniques Discussions

Calibration of the DSCOVR EPIC visible and NIR channels using MODIS and EPIC lunar observations

Igor V. Geogdzhayev[1], Alexander Marshak[2]

[1]Department of Applied Physics and Applied Mathematics, Columbia University/ NASA Goddard Institute for Space Studies, New York, NY 10025, USA
[2]NASA Goddard Space Flight Center, Greenbelt, MD, 20771

Correspondence to: Igor Geogdzhayev (igor.v.geogdzhayev@nasa.gov)

Abstract. The unique position of the Deep Space Climate Observatory (DSCOVR) Earth Polychromatic Imaging Camera (EPIC) at the Lagrange 1 point makes an important addition to the data from currently operating low orbit Earth observing instruments. EPIC instrument does not have an onboard calibration facility. One approach to its calibration is to compare EPIC observations to the measurements from polar orbiting radiometers. Moderate Resolution Imaging Spectroradiometer (MODIS) is a natural choice for such comparison due to its well-established calibration record and wide use in remote sensing. We use MODIS Aqua and Terra L1B 1km reflectances to infer calibration coefficients for four EPIC visible and NIR channels: 443 nm, 551 nm, 680 nm and 780 nm. MODIS and EPIC measurements made between June 2015 and June 2016 are employed for comparison. We first identify favorable MODIS pixels with scattering angle matching temporarily collocated EPIC observations. Each EPIC pixel is then spatially collocated to a subset of the favorable MODIS pixels within 25 km radius. Standard deviation of the selected MODIS pixels as well as of the adjacent EPIC pixels is used to find the most homogeneous scenes. These scenes are then used to determine calibration coefficients using a linear regression between EPIC counts and reflectances in the close MODIS spectral channels. We present thus inferred EPIC calibration coefficients and discuss sources of uncertainties. The Lunar EPIC observations are used to calibrate EPIC O2 absorbing channels (688 nm and 764 nm) assuming that there is a small difference between moon reflectances separated by 10 nm difference in wavelength and the calibration factors of the red (680 nm) and near-IR (780 nm) are known from comparison between EPIC and MODIS.

1 Introduction

The Deep Space Climate Observatory (DSCOVR) occupies a unique location among Earth-observing instruments in the Lagrange point L1 between the Sun and the Earth at about 1.5 million kilometers from Earth. This position allows DSCOVR Earth Polychromatic Imaging Camera (EPIC) to view the entire sunlit Earth's hemisphere (Fig. 1). Since the launch in June 2015 EPIC provided regular Earth images in ten narrow spectral channels ranging from UV to near IR. The Earth-observing geometry of the EPIC instrument is characterized by nearly constant scattering angle between 168.5° and 175.5° (Fig.2). In that EPIC's viewing geometry differs significantly from instruments on sun-synchronous orbits which rarely view Earth at such large scattering angles. Thanks to its position and viewing geometry, the EPIC instrument has the potential to augment

remote sensing observations in such applications as aerosol, cloud, sulphur dioxide and ozone amounts as well as vegetation properties.

The EPIC instrument does not have in-flight calibration capabilities making determining the calibration coefficients and monitoring their stability by means of vicarious calibration efforts a necessity. One approach to its calibration is to compare EPIC observations to the measurements from polar orbiting radiometers. Another is to use the images of the Moon regularly observed by the instrument.

Haney et al. (2016) investigated the calibration of EPIC Version 1 data using MODIS and VIIRS using the data aggregated on a .5x.5 degree grid with matching viewing geometry. They found that a navigation correction reduced the uncertainties in the calibration gain. The straylight correction was found to reduce the fit offsets and gains for all considered channel pairs.
Yu and Wu (2016) investigated the inter-calibration between Advanced Himawari Imager (AHI) in a geostationary orbit and VIIRS. They found strong linear relationship between the paired bands. The radiometric calibration between the two instruments was shown to agree within 5%.

In this study we use Moderate Resolution Imaging Spectroradiometer (MODIS, King et al., 2003), Level 1b reflectances and collocated EPIC measurements to derive the calibration coefficients in four EPIC visible and near IR (NIR) channels. We derive calibration gains for the initial (Version 1) and Version 2 releases of the EPIC data base on all available contemporaneous MODIS Aqua and Terra data. The key difference between Version 1 and Version 2 data is the applied straylight correction together with flat-fielding that made bright pixels brighter and dark pixels darker. MODIS data are a natural choice for such comparison due to their well-established calibration record and wide use in the remote sensing applications.

2 Data

EPIC L1B data were obtained from NASA Langley Atmospheric Science Data Center (ASDC). The EPIC sampling size at nadir (at the center of the image) is about 8x8 km2 (it is 10x10 km2 when the EPIC point spread function is applied) and increases towards the edges. To reduce the amount of data transmitted from DSCOVR, for all but blue channel (443 nm) four pixels are averaged on-board the spacecraft resulting in the effective spatial resolution at nadir of approximately 18 km.

We use MODIS Aqua and Terra L1B Collection 6 1-km reflectances obtained from the Level-1 and Atmosphere Archive & Distribution System (LAADS) Distributed Active Archive Center (DAAC). MODIS channels number 3, 4, 1, 2 are matched with for four EPIC visible and NIR channels: 443 nm, 551 nm, 680 nm and 780 nm, respectively, as shown in Table 1. Figure 3 shows normalized filter functions for the corresponding channels. As one can see from the figure EPIC channels are

significantly narrower compared to MODIS. The best spectral match is for the overlapping green channels, while the largest spectral difference of about 80 nm is observed between the NIR channels of the two instruments.

Two versions of EPIC data are used in this study. The initial release that covers the period between June 2015 and September 2016 will be referred as Version 1. The data from the second release (Version 2) cover the period from June 2015 and March 2017. Version 2 data include refined geolocation, flat-fielding and straylight correction algorithm. These differences require the derivation of separate sets of calibration coefficients for each of the two versions. This is discussed in more details in the "Straylight correction" section below.

EPIC channel (Full Width in nm)	**MODIS Band (Bandwidth)**
443±1 nm (3±0.6)	3 (459-479nm)
551±1 nm (3±0.6)	4 (545-565nm)
680±0.2 nm (3±0.6)	1 (620-670nm)
779.5±0.3 nm (2±0.4)	2 (841-876nm)

Table 1. EPIC-MODIS channel correspondence. (For simplicity, for the rest of the paper we will call the EPIC NIR channel 780 nm).

3 Analysis

To derive EPIC calibration coefficients we first identify favorable MODIS pixels. For each EPIC image we find MODIS pixels that match the EPIC scattering angle to within 0.5º and are temporarily collocated to within 10 min. There is a time lag in the data (Marshak et al., 2017) acquisition between different EPIC spectral channels associated with the rotation of the filter wheels: ~3 min difference between blue (443 nm) and green (551 nm), ~4 min between blue and red (680 nm). Because of that the temporal collocation is done separately for each spectral channel. We limit the solar zenith angle (SZA) of both EPIC and MODIS pixels to be no more than 60º to avoid scenes with low illumination and scenes where the curvature of the Earth may play a significant role potentially complicating the comparison. Depending on the season such favorable pixels typically occur between 30S and 30N. We ignore the EPIC pixels that are affected by specular component, (Marshak et al., 2017). We then select EPIC pixels that have a minimum of 40 MODIS pixels within 25 km radius. Relative standard deviation (defined as the ratio of the absolute standard deviation to the mean) is then calculated for the matching MODIS and EPIC pixels. In the later case 5x5 pixel neighborhood are used to calculate the standard deviation. The value of the relative standard deviation is used to select the most homogeneous scenes.

To determine the calibration coefficients two independent methods are used: the first is based on calculating the linear regression between EPIC counts and MODIS reflectances in the closest MODIS spectral channel for the most homogeneous scenes. The second is based on finding the mean MODIS/EPIC (M/E) ratio for bright homogeneous scenes (MODIS relectances greater than 0.6).

Atmos. Meas. Tech. Discuss., https://doi.org/10.5194/amt-2017-222
Manuscript under review for journal Atmos. Meas. Tech.
Discussion started: 9 August 2017

To calculate the linear regressions we use the most uniform collocated scenes with the relative standard deviations smaller then a threshold value. Because of the time delays in data acquisition between different EPIC channels and occasional gaps in transmission the sets the number of matching MODIS pixels may differ for each regression. The threshold standard deviation is selected separately for each channel. It is reduced until the correlation coefficient of the resulting regression stops increasing or the number of matching points fall below a certain value. The resulting regressions for Version 2 data are shown in Figure 4. The relative standard deviation of MODIS and EPIC points included in the regressions was between 0.5% and 1% depending on the channel.

The second approach to deriving the regression coefficients that we employed is based on calculating the ratio of MODIS reflectance to EPIC count for all matching scenes with high reflectance and relative standard deviation less than 10%. We then select the pixels for which the MODIS reflectance is greater than 0.6. Such pixels represent between 10% and 15% of the total. These scenes are binned according to the relative standard deviation of the MODIS reflectance and the mean M/E ratio is calculated for each bin. The mean bin values are then extrapolated to the ideal case of a completely uniform scene (zero standard deviation) using a linear regression. The extrapolated value is then taken to be the calibration coefficient.

This approach assumes zero intercept value. Because the number of points contributing to the M/E ratio calculations at least three orders of magnitude greater than the number of points selected for the regression method the two may be considered to be essentially independent. The four panels of Figure 5 illustrate the M/E analysis for the four EPIC channels. Whiskers show the mean and the standard variation of the ratios in each bin. Straight lines show linear regressions. One can see that for the relative standard deviation below 10% the mean M/E values are similar for every bin, so that the extrapolated value does not differ from the mean by more than 1%. The differences in the gain coefficients calculated using the two methods is summarized in Table 2. For Version 1 data the differences between the two calibration methods are between approximately 3% for the 443 nm channel and less than 0.5% for the 780 nm channel. An improved agreement is observed for the Version 2 data, for which the differences range between 0.1% and 1.4 %.

Version 1		
EPIC Channel	Calibration coefficients published on July 16, 2016	M/E Ratio/regression difference (%)
443 nm	8.80E-6	2.79
551 nm	6.90E-6	1.98
680 nm	1.00E-5	1.01
780 nm	1.50E-5	0.41
Version 2		
EPIC Channel	Calibration coefficients	M/E Ratio/regression

	published on July 6, 2017	difference (%)
443 nm	8.34E-06	0.1
551 nm	6.66E-06	0.5
680 nm	9.30E-06	0.5
780 nm	1.435E-05	1.4

Table 2. Ratio/regression gain coefficients differences and the seasonal variability of the gain coefficients for the four EPIC channels.

4 Straylight correction effect

Compared to the initial release of the EPIC data (Version 1) the second release (Version 2) includes a number of changes such as refined data geolocation for each filter and flat-fielding (correcting for CCD irregularities). In addition, a straylight correction algorithm (based on laboratory measurements and in-flight lunar observations) is used. Straylight refers to the illumination of multiple CCD pixels by a point light source. The main causes of straylight are the diffraction and ghosting (reflections between the CCD and filter surfaces). The magnitude of the effect is different for each spectral channels and is stronger in the visible compared to the UV primarily because of the larger dynamic range in the visible. The straylight correction has a two-fold effect on the EPIC counts: it decreases the count value for dark scenes and increases it for bright scenes within the image as the total radiant energy must remain constant. This results in a smaller intercept and gain of the linear regression compared to the case with no straylight correction. A schematic illustration of the effect of the straylight correction is shown in Figure 6.

Version 1 data (no straylight correction) and Version 2 data which includes straylight corrected data can be used to evaluate the effect. The regression analysis and the M/E ratio method described above were applied to both sets. The analysis shows a 4-9% reduction in the gain coefficients for the new data compared to the initial release. Consistent with expectations the reduction is smaller for the blue and green channels compared to the red and NIR ones. This reduction is observed for gain coefficients calculated by the two methods and is consistent with the expected effect of the straylight correction. Note that in order to make the two sets comparable, the spectral correction was not applied to the Version 2 data.

Similarly, we compared the regression offsets for the two datasets. Absolute reductions of the offset coefficients are observed for all channels, consistent with the expectations. The reductions range to between 1.5 and 3.7 times illustrated in Figure 7 (see next section).

Atmos. Meas. Tech. Discuss., https://doi.org/10.5194/amt-2017-222
Manuscript under review for journal Atmos. Meas. Tech.
Discussion started: 9 August 2017

5 Spectral correction

The differences in the position and spectral width of the corresponding EPIC and MODIS channels may result in discrepancies when scenes with different spectral signatures are observed by the two instruments (Chander, 2013). In version 2 calibration to compensate for these differences we employed spectral band adjustment factors (SBAFs) which convert MODIS reflectance values to equivalent EPIC reflectance for various surface types. These factors in the form of linear regression coefficients were obtained from https://cloudsgate2.larc.nasa.gov/cgi-bin/site/showdoc?mnemonic=SBAF and are based on the analysis of SCHIAMACHY hyperspectral data (Scarino et al., 2016). In addition the minimum and maximum reflectance values were identified based on the same source. MODIS pixels were spectrally adjusted if the reflectance was within these limits using the SBAFs for the appropriate land cover type. Deep convection clouds spectral corrections were applied to scenes with reflectance higher than 0.6. To identify the land cover type for each matching EPIC pixel we use a data set developed by Channan et al (2014). The dataset is a .5x.5 degree reprojected version of the Global Mosaics of the standard MODIS land cover type data product (MCD12Q1) in the IGBP Land Cover Type Classification. Separate adjustment factors were used for MODIS Aqua and MODIS Terra data.

Table 5 shows the effect of spectral adjustment on calibration gains found using M/E ratio and regression methods. The effect is different for the two methods because of the different scenes used. While for the M/E ratio analysis bright scenes, assumed to be clouds were used, the regression analysis included dark scenes and scenes of intermediate brightness as well. Overall accounting for the spectral differences of the matched channels results in changes in the gains coefficients of about 1% .The strongest effect of the spectral correction of 6% in the red channel is due to the larges SBAFs of 10-15% for the scenes of intermediate brightness. Note, that, while spectral correction was not used for the Version 1 data these scenes were excluded from the analysis and did not have an effect on the Version 1 calibration coefficients. Figure 7 shows the absolute values of the regression offsets for Version 1 and Version 2 data with and without spectral correction. One can see that the implementation of the straylight correction in Version 2 reduces the offset values for all channels. In addition spectral correction in Version 2 further reduces offsets.

	Relative difference in gain coefficients , %	
EPIC channel	M/E ratio analysis	Regression analysis
443 nm	0.8	0.9
551 nm	0.1	0.5
680 nm	1.3	6.0
780 nm	1.4	1.0

Table 5. The effect of spectral adjustment on calibration gain coefficients for version 2 data. The values in the table are calculated by subtracting the gain coefficients for data with spectral correction from the corresponding coefficients for data without spectral correction and dividing the result by the former.

Atmos. Meas. Tech. Discuss., https://doi.org/10.5194/amt-2017-222
Manuscript under review for journal Atmos. Meas. Tech.
Discussion started: 9 August 2017

6 Seasonal dependence

The length of the available EPIC dataset allowed us to evaluate the magnitude of any possible seasonal dependencies in the derived calibration coefficients. In order to do that we calculated M/E ratios separately for three-month periods between September 2015 and February 2017. Data points with MODIS reflectance greater than 0.6 and EPIC and MODIS relative standard deviation less than 5% are included. The results are shown on Figure 8. One can see that there is no noticeable trend in the data and the observed differences are within the range of variation of the ratios. Longer data series would be needed to detect and account for any potential seasonal variations. The seasonal variability of the gain coefficients calculated from the data in Figure 8 is generally less than 1% (0.9% for 443nm channel, 0.6 for the 551nm, 0.4% for 680nm and 0.6% for 780nm). We also found that the seasonal variability tends to become smaller for more homogeneous scenes. Thus for higher standard deviation value of 10% the seasonal variability is approximately 2-2.5% compared to the above values of less than 1% for standard deviation of 5%.

7 Calibration of the EPIC O2 absorbing bands using full moon EPIC observations

In general EPIC instrument observes the Moon every two-three months. Several images may be acquired for each observation, each containing several hundred individual Moon pixels.

Moon reflectance R_λ increases slowly with wavelength λ; in most cases (e.g., Ohtake et al., 2010, 2013), a 10 nm difference in wavelength leads to a difference in reflectance in the range of 0.0006-0.0013 or 0.8-1.2%. Based on this, the difference in moon reflectance between the O_2 B-band (688 nm) and the 'red' (680 nm) channels as well as between the O2 A-band (764 nm) and the near-IR (780 nm) channels will be within 1.6%. We use the moon reflectance ratios $R_{688}/R_{680} = 1.008$ and $R_{764}/R_{780} = 0.984$. Since the calibration factors for 680 and 780 nm channels are known from comparisons between EPIC Earth observations and the measurements from polar orbiting radiometers, we can obtain the calibration factors for the O2 absorbing channels at 688 and 764 nm. Indeed, the ratio $F(\lambda_1,\lambda_2)$ of the moon reflectance values measured in counts/sec at two neighboring channels λ_1 and λ_2 is very stable (Fig. 9); it is 0.466±0.002 for the 688 over 680 nm ratio and 0.591±0.002 for the 764 over 780 nm one. Thus, the calibration factor K for 688 nm, can be approximated as

$$K(688) = R_{688}/R_{688}^{counts} = R_{688}/[R_{680}^{counts}\, F(680,688)] =$$
$$= [R_{688}\, K(680)]/[R_{680}\, F(680,688)] = [R_{688}/R_{680}]\, [K(680)/F(680,688)] \approx$$
$$\approx 1.008\, [K(680)/F(680,688)].$$

Similar to 688 nm the calibration factor for 764 nm can be estimated as $K(764) \approx 0.984\, [K(780)/F(780,764)]$. Here R_λ and R_λ^{counts} are the values of calibrated reflectance and measured counts per second at wavelength λ, respectively; $K(\lambda)$ is the multiplicative calibration coefficient expressed as a conversion from counts per second to reflectance at wavelength λ and the

ratio $F(\lambda_1,\lambda_2) = R_{\lambda 2}^{counts}/R_{\lambda 1}^{counts}$. Using this technique we obtained the following calibration coefficients: $K(688)$ = 2.02e-05 and $K(764)$=2.36e-05.

Note that while both absorbing and non-absorbing channel reflectance change substantially straylight corrections (up to 10%), their ratios $F(\lambda_1,\lambda_2)$ are very stable: the difference between straylight corrected data and with no correction is less than 1.5%.

8 Comparison with ROLO-derived calibration coefficients.

The Robotic Lunar Observatory (ROLO) run by the United States Geological Survey (USGS) provides radiometric calibration and sensor stability monitoring for space-based remote sensing instruments using the Moon as a reference source (Kieffer and Stone, 2005). Using the technique of the minimization of residuals between 16 EPIC moon observations from 2015-08-29, 2016-04-21, 2016-07-19 and 2016-10-14 and the reference ROLO data an independent set of calibration coefficients was developed for all 10 EPIC channels form UV to NIR (Stone, personal communication). Figure 10 presents the comparison of the six EPIC channels gain coefficients developed in this study (see second column of the Version 2 part of Table 2 and the two gain values for the absorbing channels from the previous section) with the lunar-derived values. The absolute coefficients derived by the two methods agree to within approximately 10%, with ROLO coefficients being systematically lower. In absolute terms the gain coefficients for 4 non-absorbing channels in a better agreement compared to the two O2 absorbing channels. The two calibration sets are in a much better agreement in relative spectral terms. When the gains are normalized by the green channel gain the ratios agree to about 3%. Further research is needed to account for these differences. One source of uncertainty is the solar constant value used to convert the original ROLO radiance calibration factors to reflectances.

9 Conclusions

We derived calibration coefficients for four EPIC visible and NIR channels by two independent methods using collocated MODIS Aqua and Terra scenes. The methods were applied to the initial (Version 1) and recent (Version 2) releases of the data The gain coefficients calculated using the regression method and the MODIS/EPIC ratios agree to within between 0.1% and 1.4% for the four channels. The effects of the straylight corrections were tested using the two EPIC data versions and were shown to be consistent with expectations. In addition spectral correction for comparison of the close EPIC and MODIS channels was implemented for the Version 2 data. Overall the application of the straylight and spectral corrections result in the successive reductions of the regression offset values in all channels increasing the confidence in the consistency of the calibration coefficients derivation.

Seasonal variability was estimated from over one year long data record. It was found to be less than 1% with no discernible trend.

Using EPIC Moon observations we calculated calibration coefficients for the B-band (688 nm) and the A-band (764 nm) channels. We assumed that there is a small difference between moon reflectances separated by 10 nm difference in wavelength and the gain coefficients in the adjacent red (680nm) and NIR (780nm) were used for this purpose.

The gain coefficients developed in this study were found to agree to about 10% with ones independently derived from EPIC moon views using ROLO moon observations. The agreement improves to about 3% if the relative spectral gains normalized by the green channel value.

Acknowledgments

The DSCOVR EPIC datasets were acquired from the DSCOVR project science team. The Terra and Aqua MODIS L1b data were acquired from the Level-1 and Atmosphere Archive & Distribution System (LAADS) Distributed Active Archive Center (DAAC), located in the Goddard Space Flight Center in Greenbelt, Maryland (https://ladsweb.nascom.nasa.gov/). We are grateful to Tomas Stone for providing the ROLO-derived calibration coefficients for EPIC. We would like to thank Matt Kowalewski and Marshall Sutton for help with EPIC Lunar observations.

References

Chander, G., Hewison,T., Fox, N., Wu, X., Xiong, X., and Blackwell,W. J.: Overview of Intercalibration of Satellite Instruments, IEEE Trans. Geosci. Remote Sens., 51, 1056-1080, 2013.

Channan, S., Collins,K., and Emanuel, W. R.: Global mosaics of the standard MODIS land cover type data. University of Maryland and the Pacific Northwest National Laboratory, College Park, Maryland, USA. 2014.

Haney C., Doelling, D., Minnis, P., Bhatt, R., Scarino, B., and Gopalan, A. :The calibration of the DSCOVR EPIC multiple visible channel instrument using MODIS and VIIRS as a reference. SPIE Optical Engineering + Applications, DOI: 10.1117/12.2238010, 2016.

Kieffer, H. H., and Stone, T. C.: The Spectral Irradiance of the Moon, Astron. J. 129, 2887-2901, 2005.

King, M.D., Menzel, W.P., Kaufman, Y.J., Tanré, D., Gao, B.C., Platnick, S., Ackerman, S.A., Remer, L.A., Pincus, R., and Hubanks, P.A.: Cloud and aerosol properties, precipitable water, and profiles of temperature and water vapor from MODIS. IEEE Trans. Geosci. Remote. Sens. 41, 442–458, 2003.

Marshak, A., Várnai, T., and Kostinski, A.: Terrestrial glint seen from deep space: Oriented ice crystals detected from the Lagrangian point, Geophys. Res. Lett., 44, doi:10.1002/2017GL073248, 2017.

Ohtake, M., Matsunaga, T., Yokota, Y., Yamamoto, S., Ogawa,Y., Morota, T., Honda, C., Haruyama, J., Kitazato, K., Takeda, H., Iwasaki, A., Nakamura, R., Hiroi, T., Kodama, S., and Otake, H. : Deriving the absolute reflectance of lunar surface using SELENE (Kaguya) Multiband Imager data. Space Sci. Rev. 154, 57–77, 2010.

Ohtake, M., Pieters, C.M., Isaacson, P., Besse, S., Yokota, Y., Matsunaga, T., Boardman, J., Yamomoto,S., Haruyama, S., Staid, M., Mall, U., and Green, R.O.: One Moon, Many Measurements 3: Spectral reflectance, Icarus, 226, 364–374, 2013.

Scarino, B. R., Doelling, D. R., Minnis, P., Gopalan, A., Chee, T., Bhatt, R., Lukashin, C., and Haney, C. O.: A web-based tool for calculating spectral band difference adjustment factors derived from SCIAMACHY hyperspectral data, IEEE Trans. Geosci. Remote Sens., vol. 54, no. 5, pp. 2529-2542, 2016.

Yu, F., Wu, X.: Radiometric Inter-Calibration between Himawari-8 AHI and S-NPP VIIRS for the Solar Reflective Bands. Remote Sens. 8, 165, doi:10.3390/rs8030165, 2016.

Atmos. Meas. Tech. Discuss., https://doi.org/10.5194/amt-2017-222
Manuscript under review for journal Atmos. Meas. Tech.
Discussion started: 9 August 2017

Atmospheric Measurement Techniques Discussions

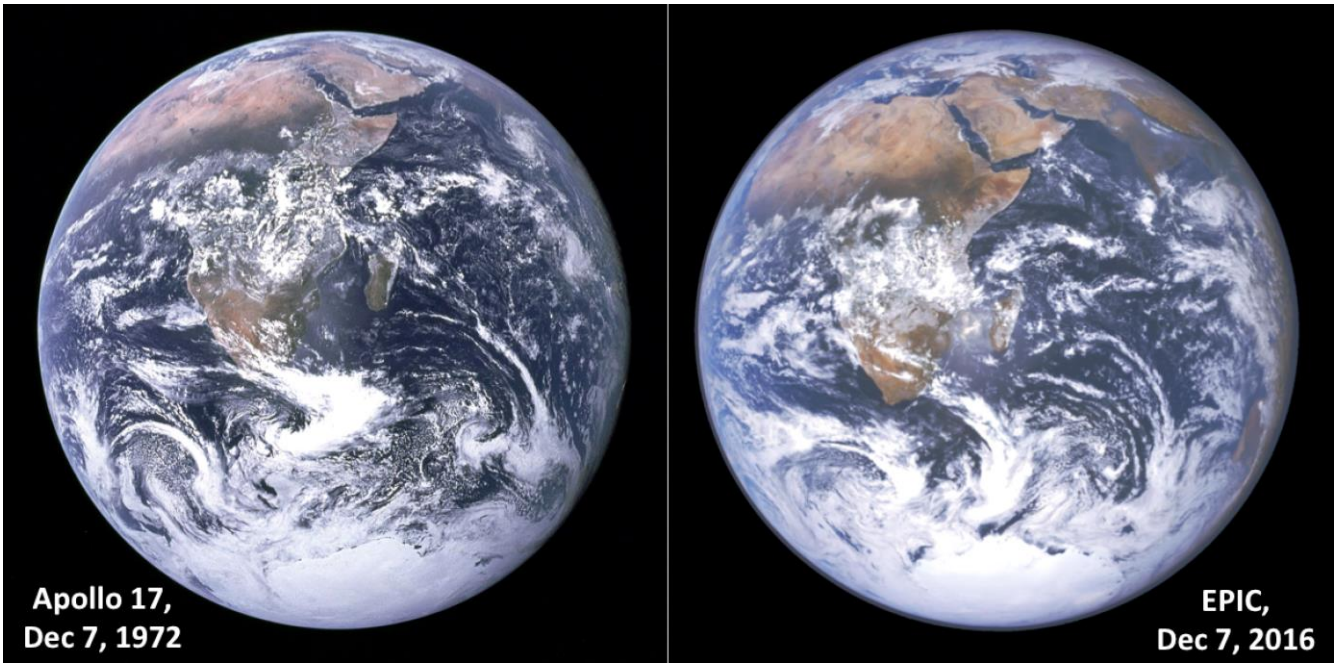

Figure 1: EPIC image of the entire sunlit Earth hemisphere (right) is compared with the APOLLO image taken on the same day 44 years ago. The two images show a remarkably similar large-scale cloud structure.

5

Atmos. Meas. Tech. Discuss., https://doi.org/10.5194/amt-2017-222
Manuscript under review for journal Atmos. Meas. Tech.
Discussion started: 9 August 2017

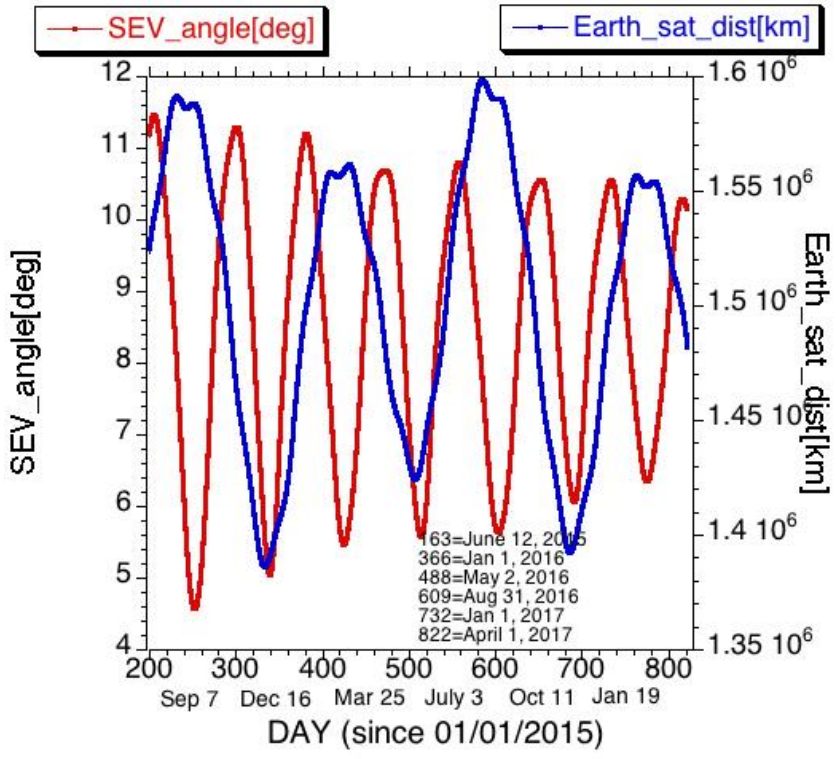

Figure 2: Solar Earth Vehicle (SEV) angle (left axis, red curve) and the distance between DSCOVR and Earth (right axis, blue curve) are plotted versus the day since January 1, 2015. Note that SEV = 180o – scattering angle between solar and viewing directions. Also note that the distance between DSCOVR and Earth changes approximately by 2000-2500 km per day.

Atmos. Meas. Tech. Discuss., https://doi.org/10.5194/amt-2017-222
Manuscript under review for journal Atmos. Meas. Tech.
Discussion started: 9 August 2017

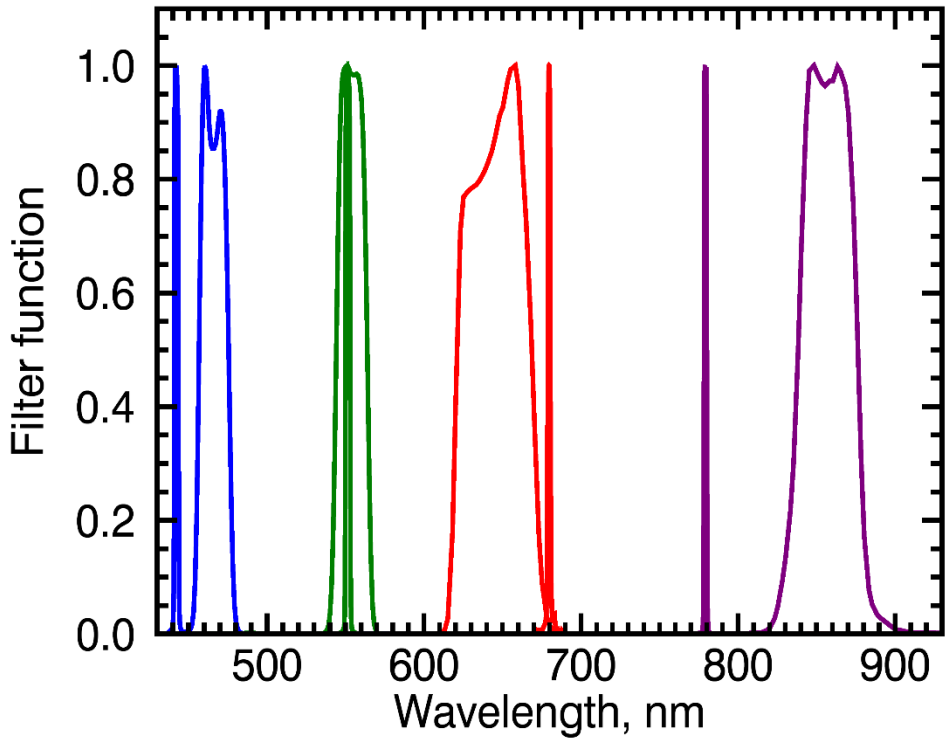

Figure 3: EPIC (narrow) and MODIS (wide) filter functions normalized to the maximum value for the four channels used in this study.

Atmos. Meas. Tech. Discuss., https://doi.org/10.5194/amt-2017-222
Manuscript under review for journal Atmos. Meas. Tech.
Discussion started: 9 August 2017

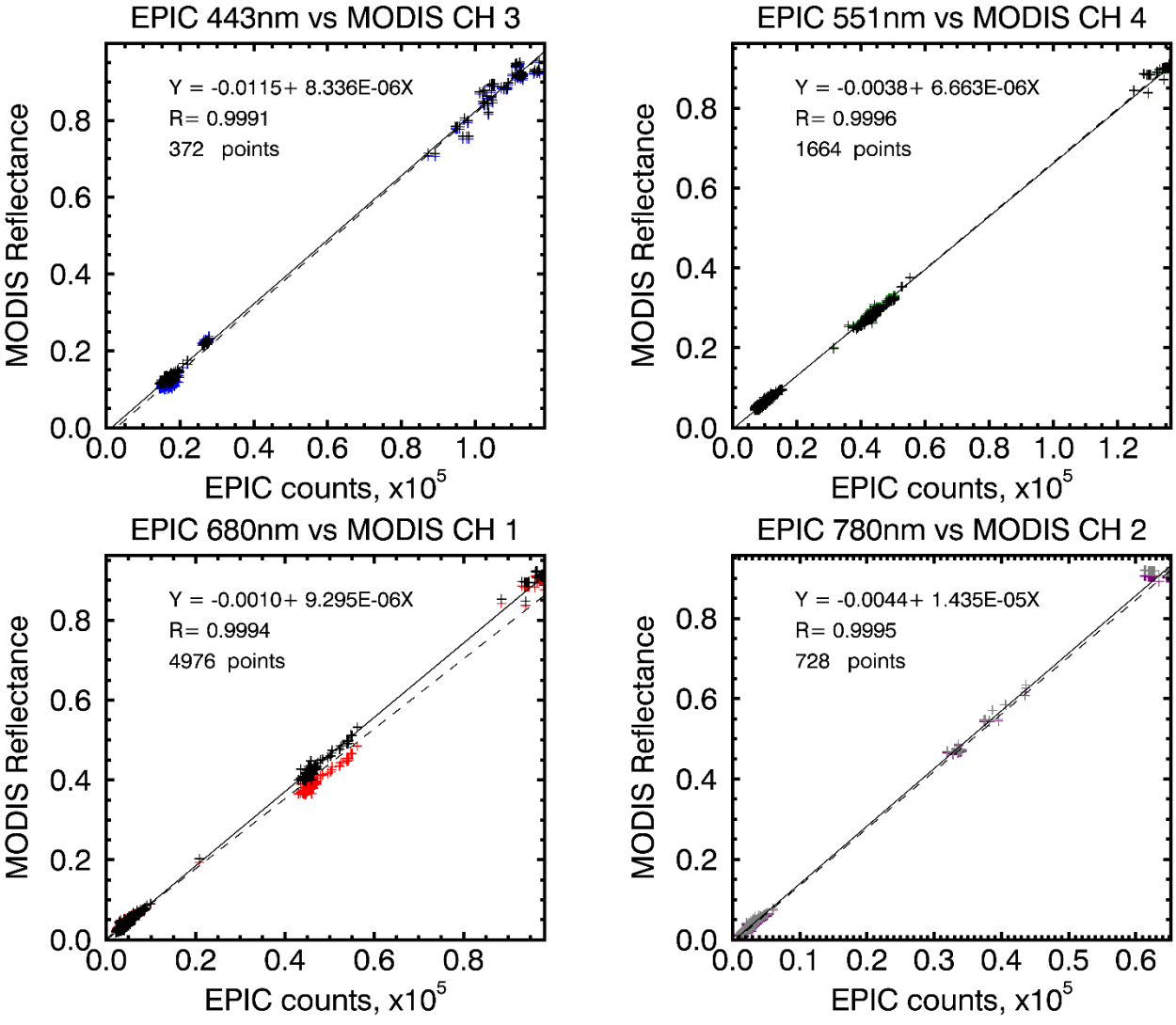

Figure 4: Scatter plots of the MODIS reflectance vs. EPIC Version 2 counts in four spectral channels for the most homogeneous matching scenes and the corresponding regression lines and equations. Also shown are correlation coefficient R and the number of points used for the regression. The colored marks and dashed lines are for the data without spectral correction, the black marks and solid lines are for data with spectral correction.

Atmos. Meas. Tech. Discuss., https://doi.org/10.5194/amt-2017-222
Manuscript under review for journal Atmos. Meas. Tech.
Discussion started: 9 August 2017

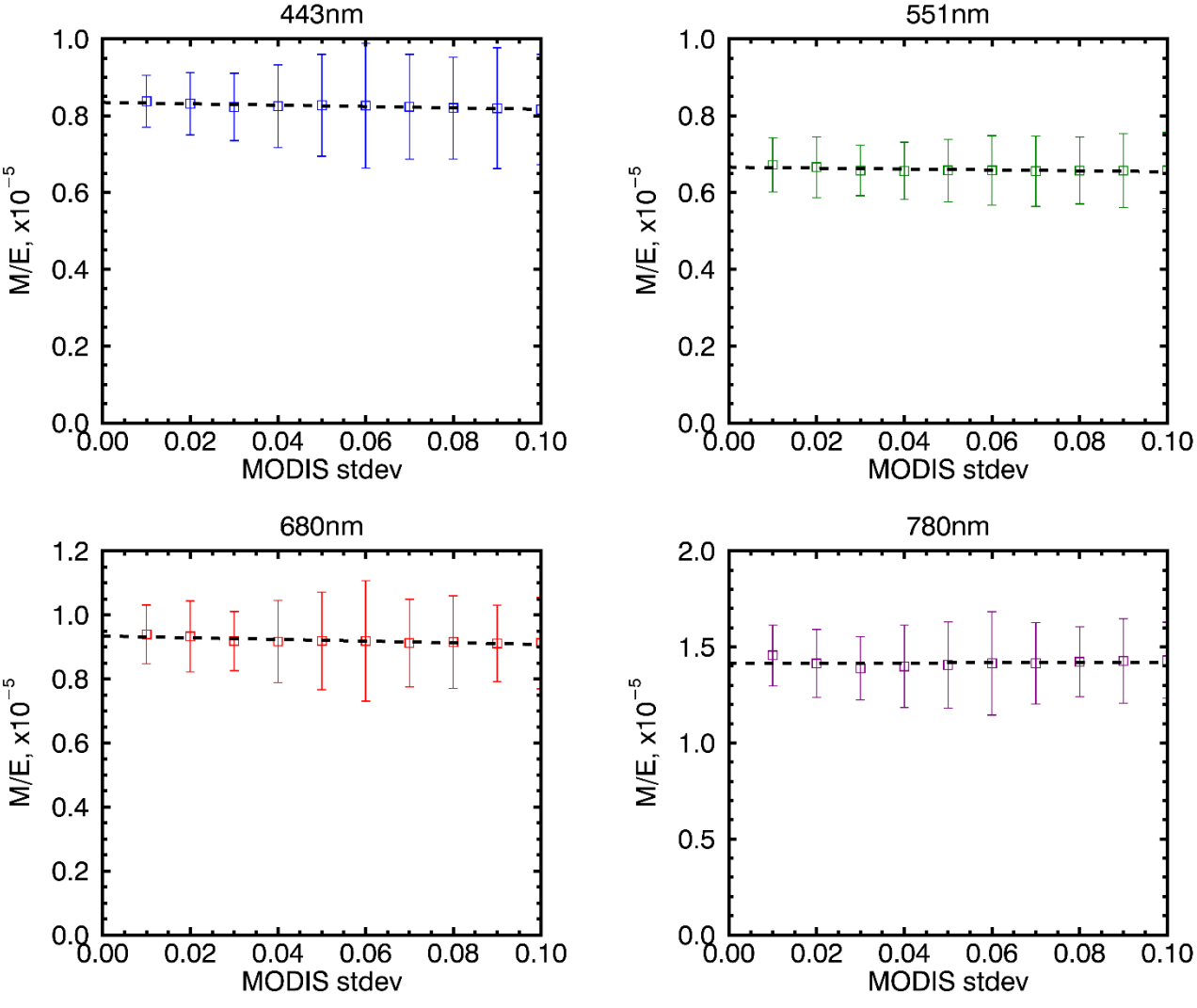

Figure 5: MODIS/EPIC ratios for the four spectral channels binned according to the MODIS relative standard deviation and MODIS reflectance >0.6. Whiskers show mean and the standard variation of the ratios in each bin. Straight lines show linear regressions. EPIC Version 2 data.

Atmos. Meas. Tech. Discuss., https://doi.org/10.5194/amt-2017-222
Manuscript under review for journal Atmos. Meas. Tech.
Discussion started: 9 August 2017

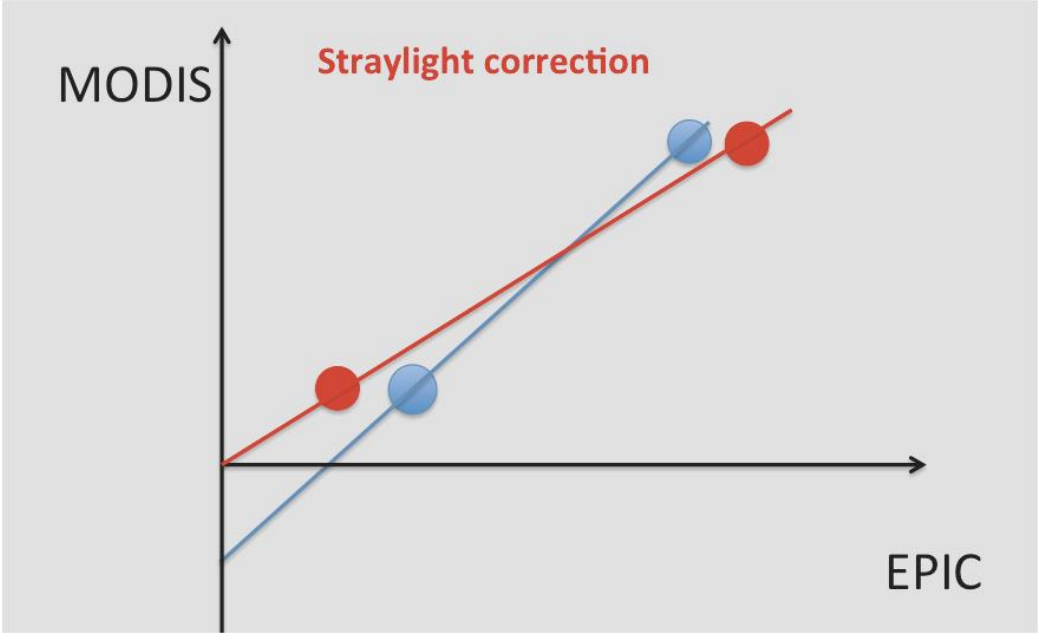

Figure 6: Schematic illustration of the effect of straylight correction. See the discussion in the text.

Atmos. Meas. Tech. Discuss., https://doi.org/10.5194/amt-2017-222
Manuscript under review for journal Atmos. Meas. Tech.
Discussion started: 9 August 2017

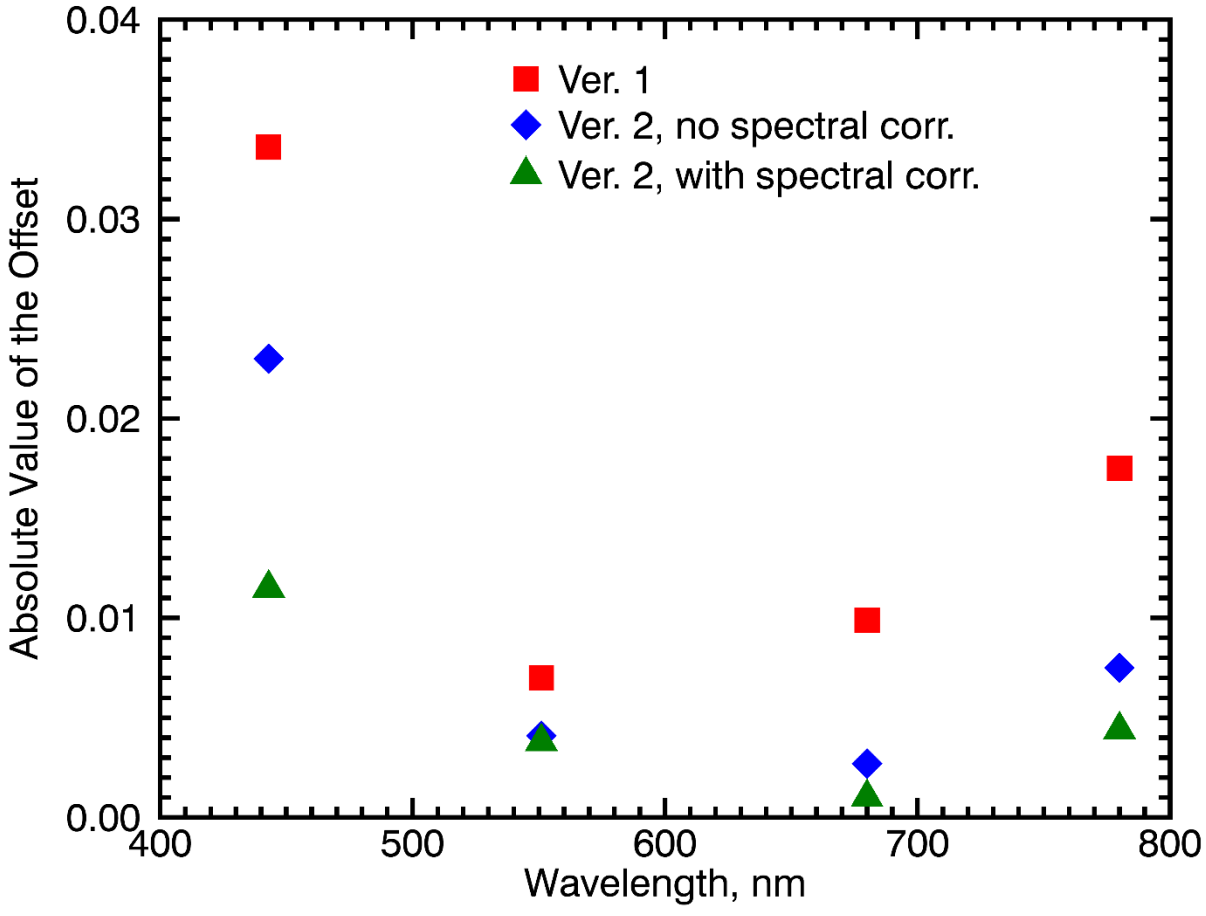

Figure 7: The absolute values of the regression offsets for Version 1 and Version 2 data with and without spectral correction.

Atmos. Meas. Tech. Discuss., https://doi.org/10.5194/amt-2017-222
Manuscript under review for journal Atmos. Meas. Tech.
Discussion started: 9 August 2017

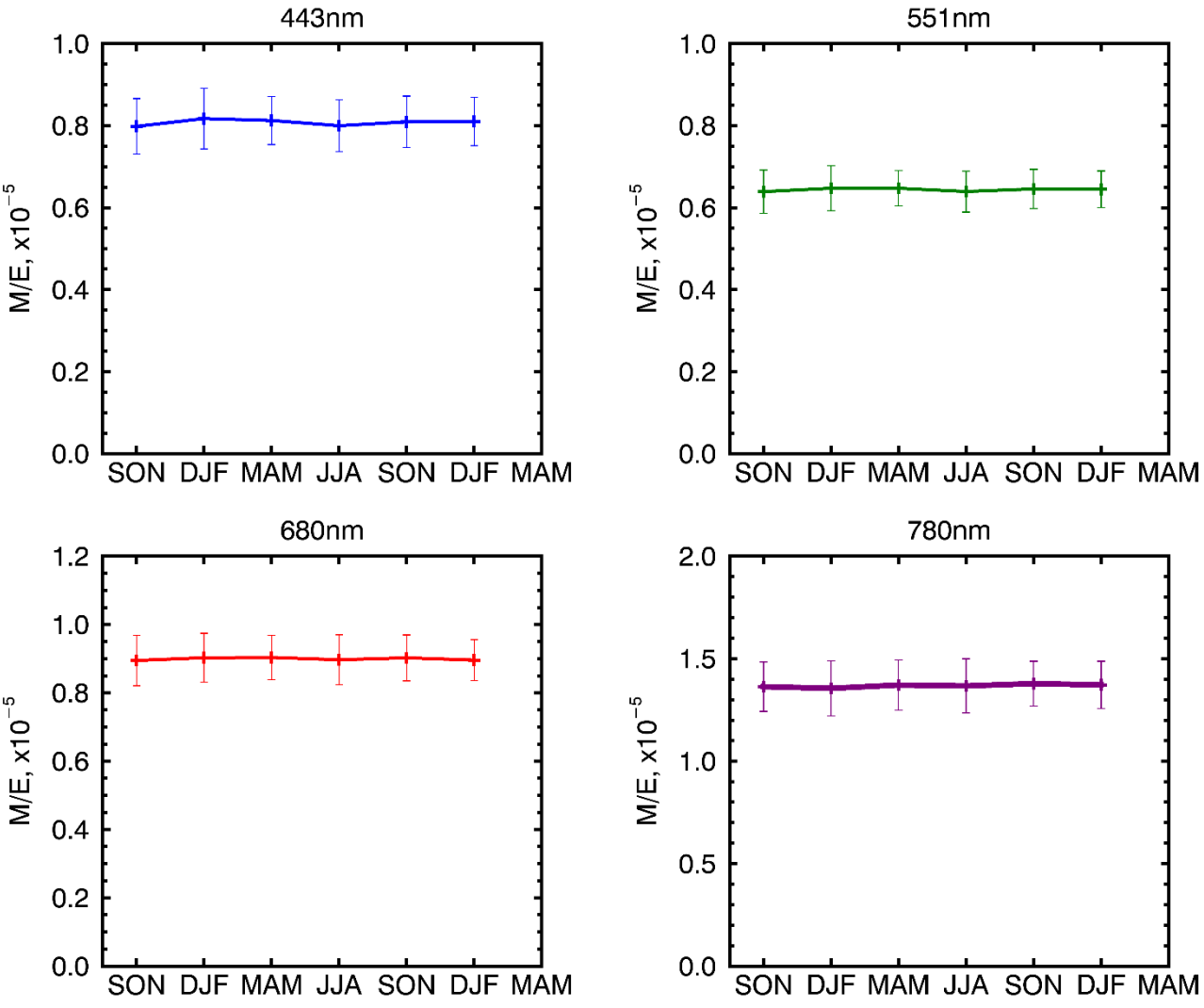

Figure 8: Seasonal dependence of the EPIC Version 2 gain coefficients from September 2015 to February 2017. Whiskers represent the standard deviation of M/E ratios within each three-month period.

Atmos. Meas. Tech. Discuss., https://doi.org/10.5194/amt-2017-222
Manuscript under review for journal Atmos. Meas. Tech.
Discussion started: 9 August 2017

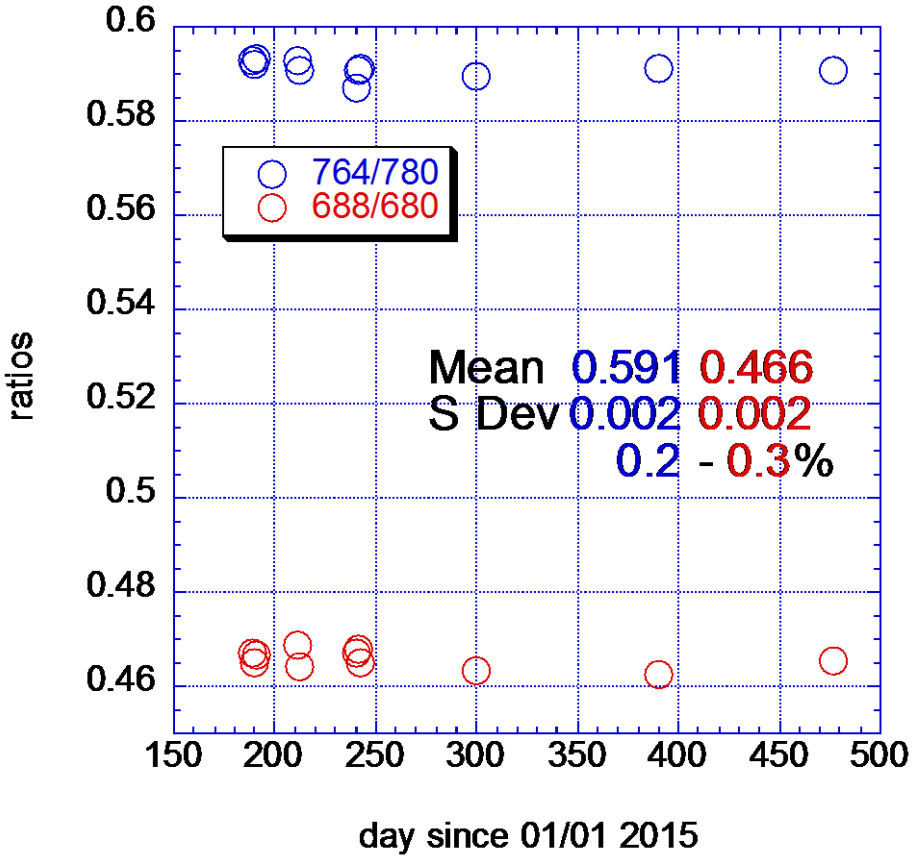

Figure 9: Ratios of O2 absorbing to reference channels using EPIC Moon observations.

Atmos. Meas. Tech. Discuss., https://doi.org/10.5194/amt-2017-222
Manuscript under review for journal Atmos. Meas. Tech.
Discussion started: 9 August 2017

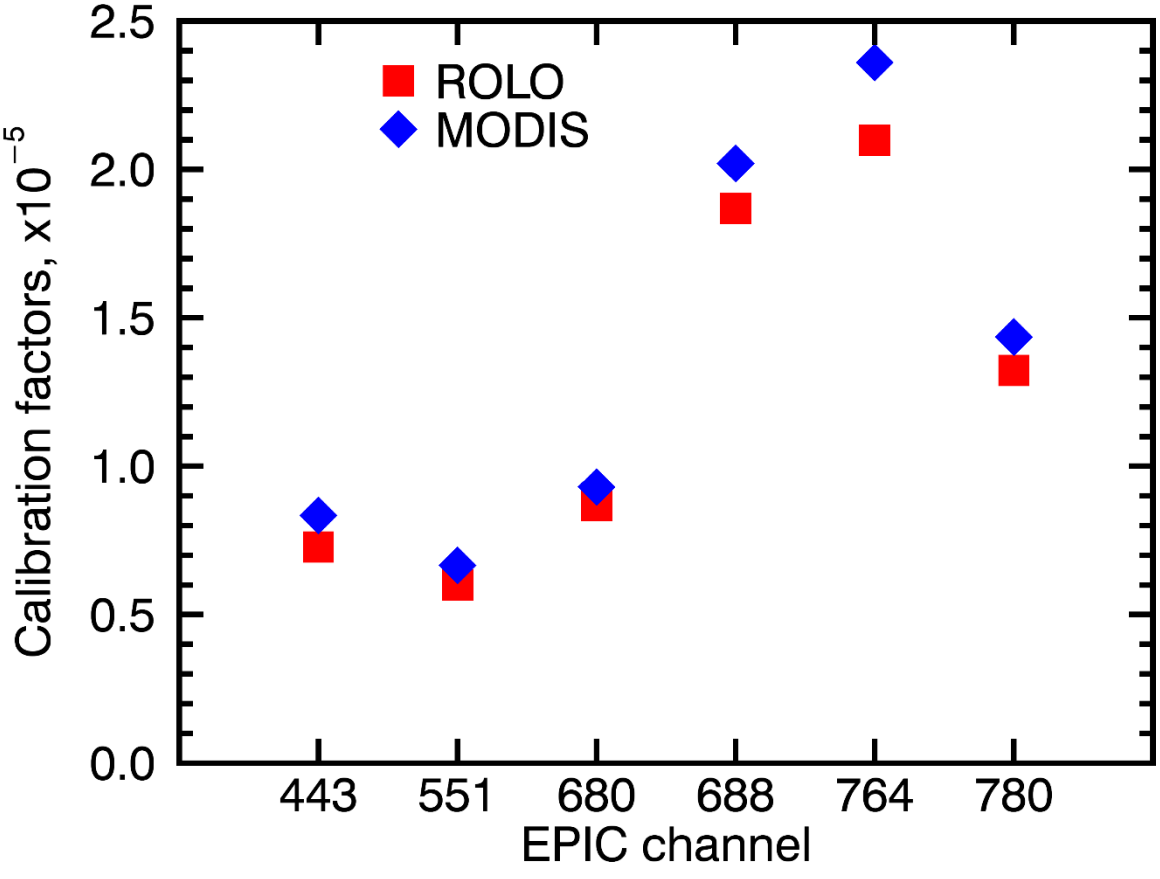

Figure 10: Comparison of MODIS- and ROLO-derived calibration coefficients.